Molecular Immunocytochemistry of the CuZn Superoxide Dismutase in Rat Hepatocytes

Ling-Yi Chang,* Jan W. Slot,‡ Hans J. Geuze,‡ and James D. Crapo*

*Departments of Medicine and Pathology, Duke University, Durham, North Carolina 27710; ‡Department of Cell Biology, Medical School of the University of Utrecht, 3511 HG Utrecht, The Netherlands

Abstract. The distribution of CuZn superoxide dismutase (SOD) molecules in subcellular organelles in rat liver hepatocytes was studied using integrated biochemical, stereological, and quantitative immunocytochemical techniques. A known concentration of purified CuZn SOD in 10% gelatin was embedded alongside the liver tissue for the calculation of CuZn SOD concentrations in hepatocyte organelles and total CuZn SOD in the rat liver. Most of the CuZn SOD was located in the cytoplasmic matrix (73.1%) and in the nucleus (11.9%) with concentrations of 1.36 and 0.71 mg/cm^3, respectively. Lysosomes contained the highest concentration (5.81 mg/cm^3). Only low concentrations were measured in mitochondria (0.21 mg/cm^3). Membrane-bound spaces of rough endoplasmic reticulum (ER), smooth ER, and the Golgi system did not contain significant concentrations of the enzyme.

By adding up the concentrations in all subcellular compartments, a total liver content of CuZn SOD was established from the immunocytochemical measurements (0.386 ± 0.028 mg/gm liver) that agreed closely with those obtained by biochemical assays (0.380 ± 0.058 mg/gm liver). The average distances between two CuZn SOD molecules can be calculated from enzyme concentrations. It was determined that CuZn SOD molecules in the cytoplasmic matrix and nucleus were 34 and 42 nm apart, respectively. In peroxisomes and mitochondria, average intermolecular distance increased to ~60 nm and increased to 136 nm in smooth ER. CuZn SOD is a relatively abundant protein in the cytosol of hepatocytes and its distribution overlaps with major sites of O_2^- production. The efficiency of protection CuZn SOD can provide to cytosolic proteins from attacks by superoxide anion depends on the rate of O_2^- production, distribution of CuZn SOD relative to cytosolic proteins, and the relative reaction rates between O_2^- with both cytosolic proteins and CuZn SOD. Future studies of these substrate-enzyme relationships in vivo can lead to a greater understanding of how cells handle oxidant stress.

THE family of enzymes called superoxide dismutases (SODs)[1] are found primarily in oxygen-using organisms (28, 32, 38, 58). These enzymes catalyse the following reaction: $2H^+ + 2O_2^- \rightarrow H_2O_2 + O_2$, and are important for the biological defense of cell injuries mediated through oxygen-free radicals. The protective role that SOD plays has been demonstrated in many ways. Tolerance to exposure to high oxygen tensions in microorganisms or in animals is closely correlated with increased cellular or tissue levels of SOD (7–9, 16–18). Conversely, a yeast mutant sensitive to oxygen was made by specifically inactivating the yeast manganese SOD gene (54). Moreover, delivery of liposome-entrapped SOD to cultured endothelial cells protects these cells against hyperoxia-induced injury (14). The mean survival time of rats exposed to 100% O_2 has also been increased by either intravenous or intratracheal injection of CuZn SOD entrapped in liposomes (30, 51). There is, therefore, compelling evidence that SODs are essential components for cellular defense against partially reduced species of O_2. The recognized biological importance of these defense systems is steadily increasing as they are implicated in processes such as ischemia-reperfusion injury (27) and aging (11, 21).

In mammalian cells, two types of SOD have been identified which have different structure and metal contents. One contains copper and zinc and the other contains manganese. Qualitative immunocytochemical localization studies carried out on ultrathin cryosections of rat liver have recently demonstrated that the CuZn enzyme is associated with cytoplasmic and nuclear matrix (46), but could not define its precise distribution in subcellular organelles. The Mn SOD is primarily confined to the mitochondria (46) but a low degree of immunolabeling is found in the cytoplasm. The intracellular distribution of the SODs would be expected to correlate with the significant sites of O_2^- production (13). The electron transport systems of mitochondria (50, 53), endoplasmic reticulum (ER) (22, 52), and nuclear membrane (59, 60) have all been shown to generate substantial amounts of O_2^-

1. *Abbreviations used in this paper*: ER, endoplasmic reticulum; RER, rough endoplasmic reticulum; SER, smooth endoplasmic reticulum; SOD, superoxide dismutase.

in vitro. A number of enzymes in the cytosol, such as xanthine oxidase and aldehyde oxidase, catalyze reactions that produce O_2^- (36). Since the superoxide anion is extremely active, it is necessary for the cell to maintain efficient defense systems to prevent O_2^--mediated damage at the site of its production.

One important aspect in the study of how cells handle oxidative stress both from normal and from abnormal production of partially reduced species of oxygen is still unknown; namely, the concentrations of the oxygen-free radical scavenging enzymes within a cell and their relation to the major sites of O_2^- production. To address this question a quantitative study aimed at defining the distribution of the CuZn SOD molecules in hepatocytes has been done by combining biochemical, stereologic, and immunocytochemical approaches and the results are reported herein.

Materials and Methods

Biochemical Assays

Three male Wistar rats weighing ~200 gm were held without food overnight and then anesthetized with sodium pentobarbital. Livers were perfused with 0.1 M PBS (pH 7.4) at an initial perfusion pressure of 15 ml/min for 1–2 min to flush out the blood. The livers were excised, weighed, and their volume determined by water displacement (39). Subsequently, each liver was homogenized in 50 mM phosphate buffer in the presence of 1% Triton X-100 using a Brinkmann Instruments Co. (Westbury, NY) polytron homogenizer. The homogenate was sonicated four times for 15 s on ice. The solubilized homogenates of liver cells were then centrifuged at 47,000 *g* for 10 min and the supernatant was removed and stored frozen. CuZn SOD activity present in the supernatant and pellet, as well as the activity in a known amount of purified rat liver CuZn SOD, were measured according to Sjostrom et al. (42). The amount of CuZn SOD present in the whole liver was calculated using the activity of the purified enzyme as a standard.

Anti-CuZn SOD Antibody

The procedures for the isolation of rat CuZn SOD and the preparation of antisera to CuZn SOD were reported previously (10, 46). Liver homogenates and the purified rat CuZn SOD were subjected to SDS-PAGE to verify the purity of the isolated protein. Homogenate protein and CuZn SOD were also applied to native gels to illustrate that all forms of CuZn SOD present in the liver homogenate are represented in the purified protein. The specificity of the anti-CuZn SOD antibody was examined by reacting the antibody to Western blots of liver homogenate, purified Mn SOD, and purified CuZn SOD. The ability of the antibody to react with all active forms of CuZn SOD was verified on Western blots of liver homogenate and purified CuZn SOD from the native gels. Moreover, the antisera was absorbed with purified CuZn SOD using Act-ultrogel (LKB Instruments, Inc., Gaithersburg, MD) coupled to the purified enzyme. Absorbed antisera was then applied to ultrathin cryosections to test the labeling specificity of the antibody on tissue sections. To test whether all the immunologically detected CuZn SOD in liver would show up in the biochemical assay, liver homogenate, and purified CuZn SOD with known amounts of CuZn SOD activity were incubated with the antisera at 4°C overnight. The antibody-antigen complexes were precipitated by incubation with *Staphylococcus aureus* (Calbiochem, San Diego, CA). The CuZn SOD activity remaining in the supernatant was assayed.

Morphometric Analysis

Livers of fasted Wistar rats were fixed by perfusing 2% glutaraldehyde (15 ml/min) in 0.1 M phosphate buffer (pH 7.4) through the portal vein for 10 min. The weight and volume of each liver were determined. Stereologic methods used in this investigation were essentially identical to those reported by Bolender et al. (5). A stratified sampling procedure was used. The volume fraction of the liver parenchyma was determined on 5 μm cryosections of the right liver lobe. The volume fractions of hepatocytes and subcellular organelles were determined on electron micrographs of Epon 812–embedded liver tissue at 10,000× and 45,000×, respectively.

Quantitative Immunocytochemistry

SOD Standards. Experiments were carried out to establish a standard curve relating labeling density on ultrathin cryosections and enzyme concentration in the embedded blocks. Blocks for standards contained multiple bands of 10% gelatin each containing a different specific enzyme concentration (0, 1, 2, or 4 mg/ml) (33, 34). The blocks were embedded in polyacrylamide according to procedures reported by Slot and Geuze (43) before cryoultramicrotomy and immunocytochemical labeling. Electron micrographs taken at 20,000× from each band of enzyme were used to determine the labeling density (number of gold particles per unit area). Finally, an en bloc enzyme standard embedded and cut alongside the tissue was used to calculate enzyme concentrations in tissue samples. This en bloc standard was required because fluctuation of labeling density could occur over time due to a variety of factors including changes in the binding property of the protein A–gold complex (33, 34). The same preparation of purified CuZn SOD was used as a standard for both the biochemical and the immunocytochemical studies.

Cryomicrotomy and Immunocytochemical Labeling. Ultrathin cryosections were obtained from composite blocks containing multiple bands of SOD or tissue with the SOD standard. Each block was mounted on a specimen holder and positioned so that a section would contain all the layers. The specimens were frozen in liquid nitrogen and ultrathin cryosections were prepared with a Porter Blum ultramicrotome equipped with cryoattachments. The sections were immunolabeled with rabbit anti-rat CuZn SOD and 9-nm protein A–gold following procedures described by Slot and Geuze (44, 45). Ultrathin cryosections were stained with uranyl acetate in methyl cellulose according to Tokuyasu (49) and modified by Griffiths et al. (20).

SOD Concentration in Tissue. Three blocks from each of the three rat livers were sectioned and labeled along with their respective en bloc SOD standard. One section from each block was examined and photographed. At a low magnification (1,000×), the entire grid was scanned from top to bottom and left to right until a grid square covered by a portion of the section free of folds was found. The grid was then moved so that the photographic frame was situated at the uppermost corner of the grid square. The magnification was then changed to 19,000× and a series of micrographs taken starting from a random spot previously selected at 1,000×. Subsequent fields were chosen by turning the horizontal stage control a quarter turn each time. When the grid bar was reached, the vertical stage control was turned an equal distance to a lower portion on the section. Sampling continued again horizontally in the reverse direction. Not every frame selected could be photographed since obliteration of structure by random events such as stain precipitation occasionally occurred. After the entire grid square was photographed, scanning at the low magnification resumed until another portion of the section free of folds was located. 30 to 45 pictures of hepatic tissue were recorded on 70-mm film and 20 to 25 photographs were taken from the area of the SOD standard. All micrographs were printed on 8″ × 10″ photographic paper at 60,000× with the aid of a calibration grid. Pictures were placed under an overlay containing 100 points spaced 2.2 cm apart (55). For liver hepatocytes, the points falling on nucleus, cytoplasmic matrix, mitochondria, cisternae of the rough ER (RER) and the Golgi complex, vesicles of the smooth ER (SER), lysosomes, and peroxisomes were tallied with a hand counter. The number of gold particles appearing on these structures were also counted and recorded. For the en bloc SOD standard, the number of gold particles appearing and the total number of points falling on each picture were recorded. Pictures were also taken from areas of gelatin around the liver tissue but away from the SOD standard to estimate background labeling. Particle and point counts from all the micrographs of one section were added and a particle to point ratio obtained. Particle counts over both hepatocyte organelles (LD^S) and the SOD reference (LD^R) were corrected for background labeling. Since labeling density was proportional to SOD concentration and the concentration in the CuZn SOD reference was known (C^R), the amount of CuZn SOD present in a unit volume of any given hepatocyte organelle (C^S) can be calculated by the following equation: $C^S = C^R(LD^S/LD^R)$.

Results

Biochemistry

The rat livers used for biochemical assays had an average weight of 5.7 ± 0.2 gm. Greater than 98% of the total CuZn SOD activity in the liver homogenate was found to associate with the supernatant after centrifugation. Total SOD content

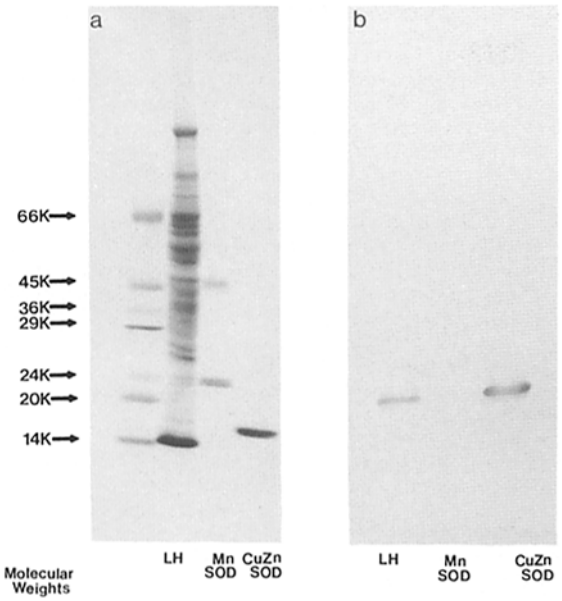

Figure 1. Specificity of the CuZn SOD antisera as demonstrated on Western blots of liver homogenates (*LH*), purified Mn SOD, and purified CuZn SOD. The proteins were separated on a SDS-polyacrylamide gradient gel (10–20%) and transblotted onto nitrocellulose paper. One set of the blots was stained for protein with Amido black (*a*). The results are demonstrated on the left with molecular weight markers. The other set of blots were incubated first with rabbit anti-rat CuZn SOD and then with goat anti-rabbit IgG conjugated with horseradish peroxidase (*b*). Hydrogen peroxide and 4-chloro-1-naphthol were used as color development reagents. The results are shown in the right panel.

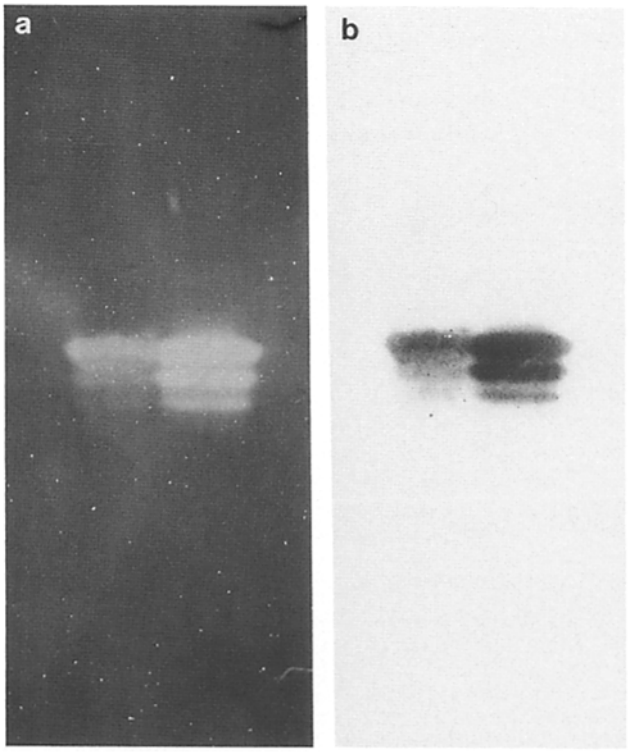

Figure 2. Purified rat liver CuZn SOD (15 μg protein) and liver homogenate (250 μg protein) applied to 10% native PAGE. (*a*) The gel was stained by a photochemical method to demonstrate SOD activity. Three strong activity bands were demonstrated by the purified CuZn SOD. The same bands were seen with the liver homogenates. (*b*) Anti-CuZn SOD antibody reaction with transblotted pure CuZn SOD and liver homogenate from native gels.

was 3.5 ± 0.4 mg per liver. The relative activity of both the CuZn SOD and Mn SOD was calculated according to the pH-dependent change of SOD activity (42). It was found that the average CuZn SOD content per liver was 2.2 ± 0.3 mg (62%) and the average Mn SOD content per liver was 1.3 ± 0.1 mg (38%). Rat liver contains, on average, 0.380 ± 0.058 mg CuZn SOD per gram of liver.

Purified Rat CuZn SOD and Anti-CuZn SOD Antibody

Although SDS gel electrophoresis of purified CuZn SOD showed only one protein band (Fig. 1), activity staining of native gels of the purified protein demonstrated three active bands (Fig. 2). The same three active bands were found with liver homogenates. The activity of Mn SOD in the liver homogenates was not demonstrated since all SOD activities were cyanide sensitive. Staining of 10% native gels of purified Mn SOD with Coomassie Blue consistently failed to show any protein band in our hands. We believe that the Mn SOD tetramer did not enter the 10% slab gel, but a 10% gel is required to resolve the different bands of CuZn SOD. The specificity of the antibody against rat CuZn SOD is shown in Fig. 1. Immunostaining of rabbit anti-rat CuZn SOD against transblotted liver homogenate protein showed a single band identical to the reaction between anti-CuZn SOD and purified rat CuZn SOD while purified rat Mn SOD exhibited no reaction with the antibody. Furthermore, absorption of the antisera by the purified antigen abolished the protein A-gold labeling on tissue sections (Fig. 3). The antisera reacts against all three active forms of the CuZn SOD (Fig. 2). Incubation of purified CuZn SOD with the antisera followed by immunoprecipitation eliminated 90% of the CuZn SOD activity of both the liver homogenate and the purified protein. Table I summarizes the experiment and results. Liver homogenate prepared with 1% Triton X-100 contained greater amounts of protein and CuZn SOD activity per unit volume than the homogenate prepared in the absence of the detergent. However, the percentages of immunoprecipitable enzyme activity from either preparation of the homogenate were the same.

Morphometry

The results of the morphometric study showed that the volume density of hepatic parenchyma is 0.87 ± 0.03 in Wistar rat liver. Hepatocytes occupied 72.3 ± 4.0% of the hepatic parenchyma. Other hepatic cells and extracellular spaces contributed 5.4 ± 1.0% and 23.3 ± 3.6% of the parenchymal volume, respectively. The absolute volumes of hepatocyte organelles were calculated using the series of volume density measurements and the fluid displacement volume of the livers. Volume densities and absolute volumes of hepatocyte

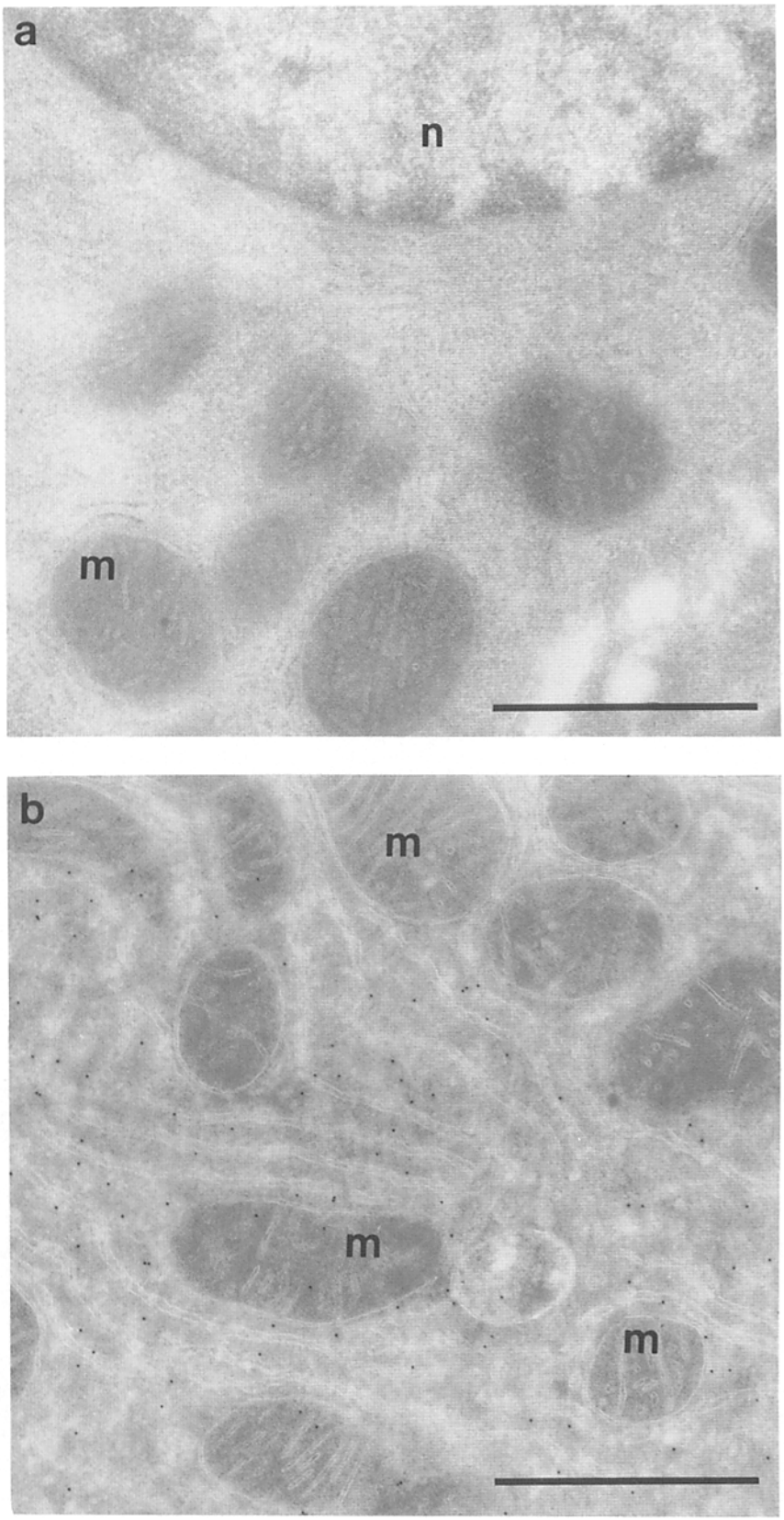

Figure 3. (*a*) An ultrathin cryosection incubated with CuZn SOD–absorbed antisera followed by protein A–gold. Only background level of gold labeling was observed. No label is found in the nucleus (*n*), mitochondria (*m*), or the cytosol. (*b*) An ultrathin cryosection labeled with Protein A–gold particles after incubation with anti-CuZn SOD antisera. Gold label is seen mainly over cytoplasmic matrix and are also found in the mitochondria (*m*). See also Fig. 6 for detailed distribution of gold labels. Bars, 0.2 μm.

Table I. Immunoprecipitation of CuZn SOD Activity

	n	Protein*	Antisera*	CuZn SOD activity	
				Original	After precipitation
			μl		
Purified CuZn SOD	3	10 μg	150	30.4 ± 1.2	3.4 ± 0.4
Liver homogenate without Triton	3	22 mg	150	38.0 ± 1.6	3.7 ± 0.8
Liver homogenate with 1% Triton	3	29 mg	150	54.0 ± 4.2	4.6 ± 0.9
Liver homogenate with 1% Triton	3	29 mg	0	52.5 ± 5.7	54.0 ± 6.2

* Mixed with 50 mM phosphate buffer to a final volume of 1 ml.

organelles are reported in Table II. The results of this morphometric study on the volume densities of hepatocyte organelles are similar to those obtained by Blouin et al. (4).

Quantitative Immunocytochemistry

Labeling Density and SOD Concentration. Polyacrylamide was used to limit antigen–antibody reactions and protein A–gold labeling to the surface when examining the relationship between labeling density and antigen concentration (34). Labeling densities for four different SOD concentrations were determined. The results from three separate experiments are plotted in Fig. 4. A constant relationship between the number of gold particles per unit area and the corresponding SOD concentration was demonstrated. These labeling studies were carried out within a span of 3 wk with the same preparation of 9-nm protein A–gold. A separate test with a different batch of protein A–gold demonstrated the same linear relationship but a slightly different ratio between label and concentration.

Table II. Hepatocyte Organelle Volumes by Morphometry

Hepatocyte organelles	Volume density* of organelles in hepatocytes	Organelle volumes‡ (cm^3/g liver)
Nucleus	0.111 ± 0.034	0.064 ± 0.022
Cytoplasmic matrix	0.364 ± 0.028	0.210 ± 0.026
Mitochondria	0.276 ± 0.026	0.158 ± 0.007
RER	0.065 ± 0.029	0.038 ± 0.019
SER	0.158 ± 0.046	0.090 ± 0.023
Golgi apparatus	0.002 ± 0.001	0.001 ± 0.001
Lysosomes	0.006 ± 0.002	0.004 ± 0.001
Peroxisomes	0.012 ± 0.002	0.007 ± 0.001

* Mean volume of livers, 6.52 ± 0.28 cm^3; mean volume density of hepatocytes in liver, 0.63 ± 0.04; mean weight of livers studied, 6.85 ± 0.56 g.
‡ Calculation of volume was carried out for each section. Three measurements were made for each rat and averaged. The mean and SD were then calculated from the three individual animal values.

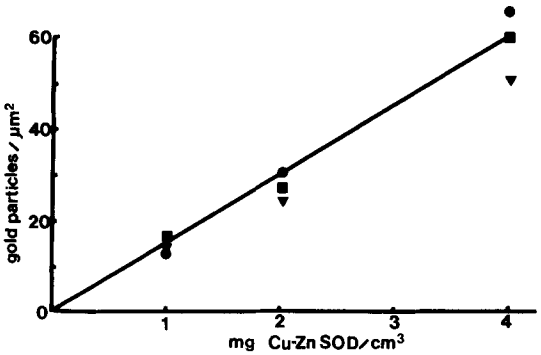

Figure 4. Labeling densities (number of gold particles/μm^2) of the purified CuZn SOD at various concentrations. The amount of background (0 mg CuZn SOD/ml) labeling was <1% of that of 1.0 mg CuZn SOD/ml. Results from three experiments, after substrating the background staining (●, ■, ▼).

Distribution of CuZn SOD. CuZn SOD was found in all liver cells, but the hepatocytes were the most densely labeled cells. Extracellular spaces were not labeled. Fig. 5 illustrates the density of gold labels on an endothelial cell in comparison with that found over the cytoplasm of an adjacent hepatocyte. The number of gold particles found per unit area of endothelial cell cytoplasm was ~1/4–1/3 of that found on a typical hepatocyte. Kupffer cells and the fat-storing cells had roughly the same labeling density as endothelial cells.

The distribution of CuZn SOD within the hepatocyte was found to be identical to that described by Slot et al. (46), although the labeling density was greatly diminished due to blockage of penetration by polyacrylamide. Fig. 6 demonstrates the distribution of labeling of CuZn SOD in the cytoplasm. Protein A–gold labeling was observed in the nucleus and in the cytoplasmic matrix. Virtually none was found within the vesicles and cisternae of the ER or the Golgi complex. Lysosomes, on the other hand, were densely labeled. A low but consistent amount of gold labeling was located over mitochondria and peroxisomes.

The Concentration of CuZn SOD in Subcellular Organelles. As described in Materials and Methods, the concentration of CuZn SOD in various subcellular organelles was determined by comparing the labeling densities to that of a SOD standard. The labeling density of CuZn SOD in 10% gelatin at a concentration of 1 mg/ml ranged from 12 to 22 gold particles per μm^2 and averaged 14.3 ± 3.2/μm^2. The level of background labeling stayed fairly consistent, ranging from 0.3 to 0.5 gold particles per μm^2. Determination of organelle SOD concentration on any given section is calculated from the labeling density of the SOD standard on the same section and was also corrected for background using measurements from the same section. Variations between sections from the same animal range from 5–8% of the mean for nucleus and the cytosol to 30–50% of the mean for sparsely labeled compartments like the Golgi complex and ER. Variation for mitochondrial labeling from section to section was ~10% of the mean. Table III reports the concentrations of CuZn SOD in the major hepatocyte organelles. The highest concentration was found in lysosomes. CuZn SOD was four times more concentrated in lysosomes than in cytoplasmic ground substance and eight times more so than in

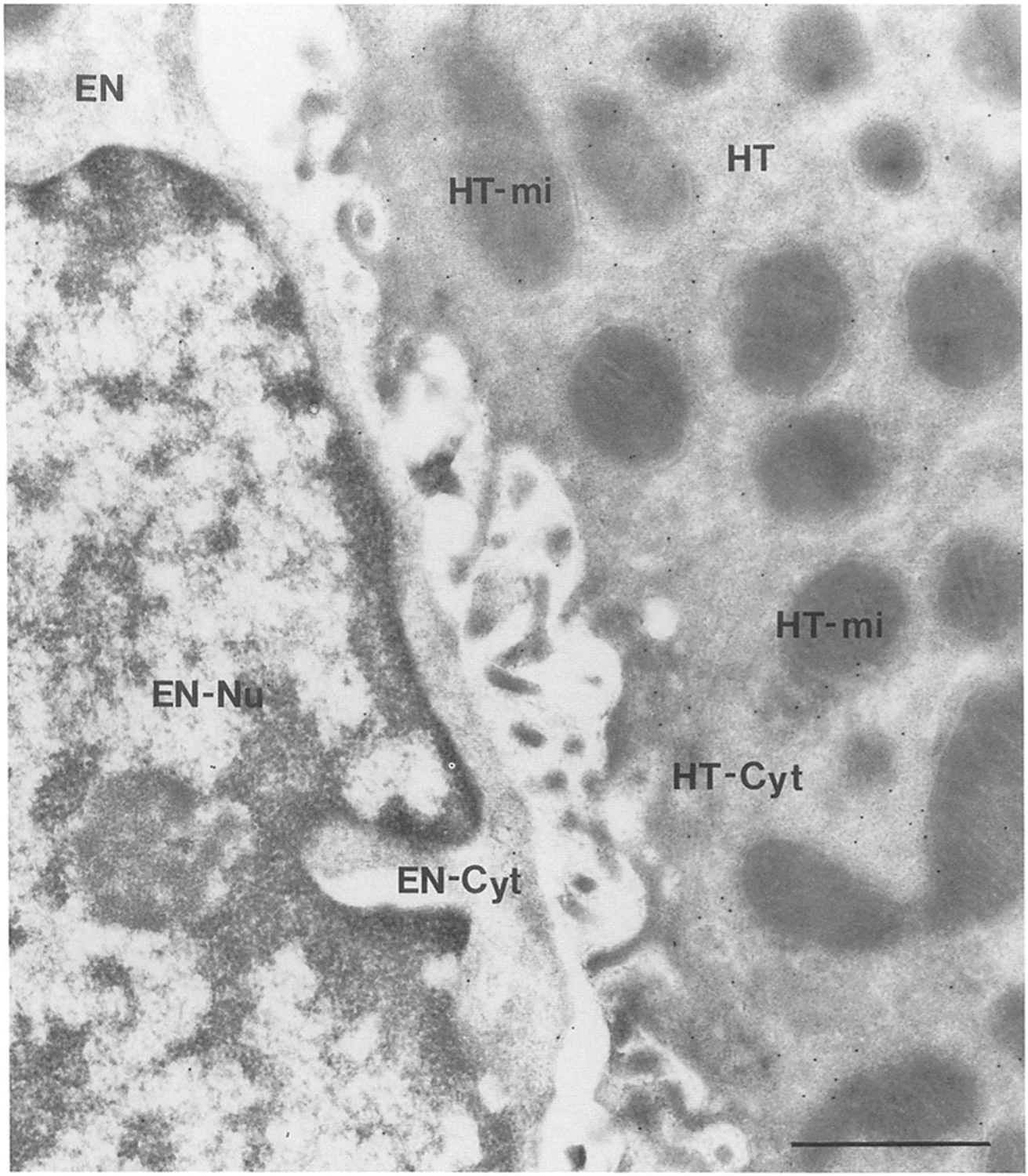

Figure 5. Comparison of CuZn SOD immunolabeling on an endothelial cell (*EN*) with that of an adjacent hepatocyte (*HT*). The nucleus (*EN-Nu*) and the cytoplasm (*EN-Cyt*) of the endothelial cell are sparsely labeled, whereas the cytoplasm of the hepatocyte (*HT-Cyt*) on the right shows a much higher labeling density. *HT-mi*, hepatocyte mitochondria. Bar, 1 μm.

the nucleus. Mitochondria and peroxisomes exhibited 20–25% of the cytoplasmic SOD concentration. The cisternae and vesicles of the RER, SER, and the Golgi complex contained little or no CuZn SOD.

CuZn SOD in Hepatocyte Organelles and Total CuZn SOD in the Liver. To calculate the relative content of SOD in each of these organelles within the liver, the volume (cm^3/gm liver) of the organelle was multiplied by the con-

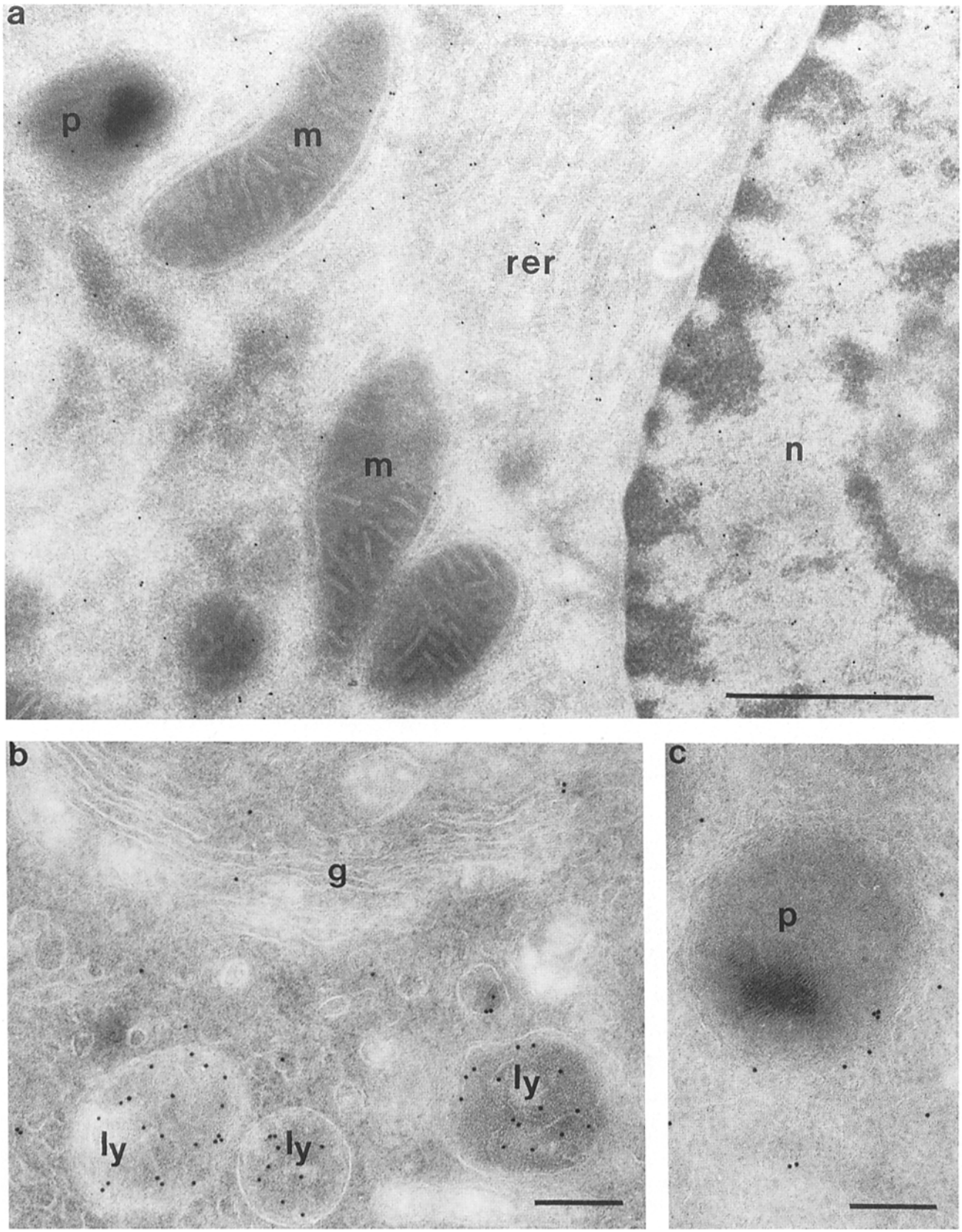

Figure 6. Immunolabeling of CuZn SOD on hepatocyte cryosections of rat liver (*a*). Protein A–gold labeling of CuZn SOD is observed mainly in the matrix of nucleus (*n*) and cytoplasm. Small amounts of label are found on the mitochondria (*m*). The cisternae of the RER (*rer*) is not labeled. (*b*) Lysosomes (*ly*) are the most heavily labeled membrane-bound organelle in the hepatocyte. The cisternae of the Golgi complex (*g*) exhibit no specific labeling. (*c*) Peroxisomes (*p*) in the hepatocyte also exhibit a low but constant labeling. Bars: (*a*) 1 μm; (*b* and *c*) 0.2 μm.

Table III. Total CuZn SOD Content in Rat Liver

Hepatocyte organelles	SOD concentration* (mg/cm³)	Total SOD content‡ (mg/g liver)
Nucleus	0.71 ± 0.06	0.046 ± 0.017
Cytoplasmic matrix	1.36 ± 0.30	0.282 ± 0.030
Mitochondria	0.21 ± 0.01	0.033 ± 0.019
RER	0	0
SER	0.02 ± 0.01	0.002 ± 0.002
Golgi apparatus	0	0
Lysosomes	5.81 ± 1.55	0.021 ± 0.010
Peroxisomes	0.27 ± 0.08	0.002 ± 0.000
Total		0.386 ± 0.028

* Calculation of concentrations was carried out for each organelle from each section using the en bloc standard. A mean concentration for each animal is determined from three measurements. The overall mean and SD from three rats are reported.

‡ Total organelle volumes and their corresponding SOD concentrations per unit volume were calculated for each rat as described under Tables II and III. Multiplication of volume with concentration then gives rise to the SOD content in the organelle. Total organelle CuZn SOD and total liver CuZn SOD were calculated for each animal. The mean and SD from three rat livers are reported.

centration of SOD. The calculations were performed for each liver and the results from three livers averaged. Table III lists the organelle contents of CuZn SOD. Adding up all organelle enzyme contents, we found that the total amount of CuZn SOD in hepatocytes is 0.386 ± 0.028 mg/gm liver. It can be seen that ~73% of the CuZn SOD in hepatocytes is located in the cytoplasmic matrix. Mitochondria and nucleus contributed 9 and 12%, respectively. Because lysosomes have a small total volume, their contribution to total SOD content is only 5.4%, despite their high enzyme concentration.

Morphometric analysis has shown that nonhepatic cells constitute ~4.7% (87% × 5.4%) of the liver mass and have a lower concentration of CuZn SOD (<1/3) than hepatocytes. It can be inferred that nonhepatocytes contribute only 2–3% of the total liver CuZn SOD or that 0.386 mg CuZn SOD/gm liver accurately reflects the total liver content of CuZn SOD. Comparison of the immunocytochemical quantification of the CuZn SOD with the biochemical assays reveals a close correlation in results for these two markedly different methods for quantification of this enzyme.

Discussion

An understanding of intracellular pool sizes of enzymes has always been of fundamental interest in the study of cell structure and function. Earlier approaches to this problem have involved measuring enzyme activities in subcellular fractions. While these methods are useful in roughly defining the distribution of biological activities, the localization of specific proteins is not precise due to the overlapping distribution of biological membranes in physically isolated fractions. The integrity of cell structure is by necessity destroyed by isolation procedures and this makes sound structure–function correlations difficult. Some organelles, such as the RER, lose their native configuration when fractionated. Moreover, cell extracts even from isolated cells invariably carry organelles from mixed cell populations, in most cases with widely different metabolic functions.

Developments in immunocytochemical techniques have made it possible to study specific enzyme distributions directly on intact cell structures (19, 34, 35). Posthuma et al. (34) recently demonstrated a new approach for quantitative immunocytochemistry with a model system of soluble proteins in gelatin. This approach has now been applied for the first time to study intracellular SOD concentrations in rat liver parenchymal cells. Independent biochemical determination of total liver CuZn SOD content demonstrates the reliability of the immunocytochemial results. Furthermore, by the integration of biochemical, morphometric, and immunocytochemical techniques, the distribution of enzyme molecules at specific subcellular sites can be studied.

One potential problem for the immunocytochemical quantitation of SOD is the possible presence of multiple forms of the CuZn SOD. Previous study by Weisiger and Fridovich (57) had shown that chicken liver CuZn SOD exists as a family of electrophoretically discrete forms. All forms of the CuZn SOD were active. It is not known whether these multiple forms are truly isozymes or whether they represent the product of a single gene variably modified by amidation or by some other posttranslational change. Three different bands exhibiting CuZn SOD activity can be demonstrated on native gels of both rat liver homogenate and the purified CuZn SOD. All three bands were reactive with the anti–CuZn SOD antibody. The anti–CuZn SOD antibody appeared to react equally with the cytosolic and membrane-contained CuZn SOD, since the same percentage of CuZn SOD activity was immunoprecipitated from the liver homogenate with or without Triton X-100. Because all detectable bands present in the liver homogenate are found with the purified protein and our antibody recognizes all forms of CuZn SOD, immunocytochemical quantitation of the CuZn SOD can be achieved.

An important assumption in this immunocytochemical study was that the purified enzyme is biochemically and immunologically similar to the in vivo form of the protein. The extensive body of literature on this enzyme supports this assumption (9, 10, 12, 15, 17, 18, 55). In addition, we have shown that an equal proportion (90%) of the CuZn SOD activity can be depleted from both the liver homogenate and the purified CuZn SOD by immunoprecipitation. The results of our quantitative study show that the total amount of hepatic CuZn SOD determined by quantitative immunocytochemical methods closely approximated that determined by biochemical techniques. This implies that the ratio between biochemically active CuZn SOD in the liver homogenate and biochemically active CuZn SOD in the purified protein is equal to the corresponding ratio of immunologically active CuZn SOD in the tissue section and in the purified protein. The simplest explanation for the similar immunocytochemical and biochemical results is that all hepatocyte CuZn SOD including those molecules located in the lysosomes are immunologically and biochemically active, and that these activities retain a constant relationship for all the isoforms. In view of the multiple localizations of CuZn SOD, other ratio relationships that can explain the present results require that all possible errors offset each other and are, therefore, less likely. The correlation between the two quantitative techniques is not surprising, since the CuZn SOD is an exceptionally stable enzyme. Whether biochemical and immunocytochemical correlation exists for the quantitation of other

enzymes will depend largely on the characteristics of the individual proteins involved.

The presence of CuZn SOD in several subcellular compartments poses some interesting questions concerning cellular addressing of the same enzyme molecules to different locations. It is possible that the different forms of CuZn SOD have different cellular localizations. This has not been demonstrated since monospecific antibodies to each of the electrophoretically distinct forms of CuZn SOD are not yet available. Presently only one gene encoding the cytoplasmic SOD has been recognized from rat (23). The enzymes catalyzing the chemical reactions of intermediate metabolism is mostly synthesized by ribosomes in the cytosol (2). While the precise site of CuZn SOD synthesis is unknown, there is no evidence to indicate that it differs from other cytosolic enzymes. Cytosolic CuZn SOD could diffuse into the nucleus through nuclear pores. CuZn SOD activity detected with isolated nuclei can be depleted through repeated buffer washes demonstrating that CuZn SOD can enter or leave the nucleus freely (56). The presence of high concentrations of CuZn SOD in lysosomes can be accounted for by the autophagic process of the hepatocyte (1, 58). It has been shown that hepatic lysosomal content of CuZn SOD increased after starvation (15). This increase coincides with a greater rate of autophagic activity during starvation. Endocytosis is a possible but not likely source of lysosomal CuZn SOD. Immunocytochemical studies of inflation-fixed (intact vascular bed) lung tissue showed a very low labeling density over plasma. Furthermore, the lysosomes of alveolar macrophages are devoid of CuZn SOD (our unpublished observations).

The mechanism of CuZn SOD packaging into the mitochondria is unknown. Mn SOD is thought to be transported into the mitochondria in an inactive form with a polypeptide signal sequence that can attach to mitochondrial proteins (41). After gaining entrance into the mitochondria, this leader sequence is cleaved. DNA sequencing of the CuZn SOD has demonstrated that this enzyme has no leader sequence (23). That a cytosolic protein like the CuZn SOD can enter mitochondria is not unique. The cytosolic antioxidant enzyme glutathione peroxidase was also found in the mitochondria of liver and adrenal cortex (48). One might speculate that the mitochondrial CuZn SOD is coded by a nuclear gene yet unrecognized or that it has a local (mitochondrial) origin. Proteins located in the peroxisomes are believed to be synthesized on free ribosomes in the cytosol (29). Most peroxisomal proteins studied to date, including the antioxidant enzyme catalase, appear to be synthesized as mature proteins and do not have a signal sequence (6, 29). Translocation of enzymes in this case could occur by secondary alterations such as cofactor binding or interaction with other organelle components (6).

The distribution of CuZn SOD activity within the cell overlaps with known sites of superoxide generation. Quantitatively important contributions to intracellular free radical production are made by soluble cell components found in both the cytoplasm and nuclear matrixes (13). High concentrations of CuZn SOD are found within these two compartments. Mitochondria have been shown to produce significant amounts of superoxide at the ubiquinone–cytochrome b region, probably due to the autooxidation of ubisemiquinone (13). NADH dehydrogenase and dihydroorotate dehydrogenase are also autooxidizable electron carriers which contribute to mitochondrial superoxide production (13, 50). However, the mitochondria scavenger of superoxide is most likely to be the Mn SOD. Biochemical analysis routinely shows that >30% of the total liver SOD activity is associated with the Mn-containing enzyme. Mn SOD has been shown to be present almost exclusively in the mitochondria (46, 57). The relatively small amounts of CuZn SOD in mitochondria are likely to play a minor role in the protection against oxidants when compared with Mn SOD. Peroxisomes contain the enzymes of the fatty acid β-oxidation system (6, 29) and could be a site of free radical production.

A high concentration of CuZn SOD was found in lysosomes (31). It is known that hepatocyte lysosomes nonselectively take up cytoplasmic proteins through an autophagic process (1, 58). Since CuZn SOD is resistant to protease digestion (12), its concentration in lysosomes may build up to a high level. It should be noted that lysosomes contributed only 5% of the total liver content of CuZn SOD (Table III).

Cytochromes P_{450} and b_5 on the ER and on nuclear membranes have been shown to be capable of producing significant quantities of superoxide under hyperoxic conditions (13, 52), while the cisternae of both SER and RER contain very low concentrations of CuZn SOD. Cytochrome P_{450} has been described as protective itself in oxygen toxicity owing to its peroxidase activity (26). It has been reported that induction of pulmonary and liver cytochrome P_{450} using β-naphthoflavone is associated with an increase in the CuZn SOD activity in the lung (26). Kikkawa et al. (24) have argued that microsomes are an important site of oxygen radical production in pulmonary oxygen toxicity. They reported that depression of the hemoprotein of microsomes by the administration of interferon inducers is associated with protection against hyperoxia. The relative rate of O_2^- production by cytosolic and microsomal enzyme systems is not known. One explanation for the low CuZn SOD concentrations in the cisternae of SER and RER could be that the microsomal system plays a relatively minor role in superoxide production under normoxic conditions in vivo. Alternately, the O_2^- production site on the membrane of the ER could be oriented toward the surrounding cytoplasm which is rich in CuZn SOD.

An integrated system of biochemistry, stereology, and quantitative immunocytochemistry can be used to study distribution of protein molecules within the cell. We, therefore, define molecular immunocytochemistry as the combined application of stereology, quantitative immunocytochemistry, and biochemical assays to determine the total number of specific protein molecules at specific subcellular sites. Biochemical assays provide an assessment of the total functional activity of the selected protein in the target tissue. Quantitative immunocytochemistry can describe the subcellular distribution of protein molecules. Since the molecular weight of CuZn SOD is known (32,000), the distribution of enzymatically active CuZn SOD molecules can be determined (32,000 gm of CuZn SOD contains 6×10^{23} molecules). Because the total amount of rat liver CuZn SOD measured by biochemical and immunocytochemical methods were identical, the enzyme concentrations obtained by quantitative immunocytochemistry can be used directly to calculate the density of enzyme molecules. Table IV presents the distributions of CuZn SOD molecules in subcellular compartments of the hepatocytes. There are roughly 26,000

Table IV. Distribution of CuZn SOD Molecules in Hepatocyte Organelles

Subcellular compartment	Number of molecules/μm^3	Average distance between SOD molecules
		nm
Nucleus	13,300	42
Cytoplasmic matrix	25,500	34
Mitochondria	3,940	63
SER	400	136
Lysosomes	108,900	21
Peroxisomes	5,000	58

CuZn SOD molecules per μm^3 of cytoplasmic ground substance on the average or one CuZn SOD molecule is found in each 40,000 nm^3 of cytoplasm. Accordingly, the average distance between the centers of two CuZn SOD molecules in the cytosol is ~34 nm. The distance between the two copper residues in the dimeric molecule of CuZn SOD is 3.4 nm (37). The widest part of the enzyme molecule is ~6.0 nm. Therefore, the average distance between two SOD molecules in hepatocyte cytosol is 6–10 times the diameter of the molecule itself. Assuming an overall concentration of cytosolic protein of 15 g/100 ml and an average molecular weight of 100,000, there would be 900,000 protein molecules per μm^3 or an average distance of 10 nm between the centers of protein molecules. There is clearly a greater probability of a superoxide anion hitting a cytosolic protein than CuZn SOD. However, the effectiveness of the protection CuZn SOD provides to cytosolic protein components depends on both the relative collision and the relative reaction rates between O_2^-–cytosolic protein and O_2^-–CuZn SOD.

CuZn SOD has an extremely high enzyme rate constant (10^9 $M^{-1}s^{-1}$) while the naturally occurring concentrations of superoxide are very low (25). The reaction between SOD and O_2^- is therefore diffusion dependent. The association between CuZn SOD and superoxide, however, is not a simple matter of diffusion and collision. Enzyme submolecular structure, detailed electrostatic charge distribution, solvent-screened inter- and intramolecular interactions, and hydrodynamic interactions can affect diffusion of substrate as well as association of substrate with enzyme. The structure of the CuZn SOD has been studied extensively. Computer simulations of superoxide diffusion to the active site of CuZn SOD have been conducted by a number of investigators (3, 40, 47). It has been found that the electric field of the enzyme enhances the association rate of the anion by 30-fold (3). These studies are generating greater understanding of the interaction between CuZn SOD and superoxide at the level of individual enzyme molecules. Information provided by molecular immunocytochemistry describing the distribution or spacing of enzyme molecules in its in vivo microenvironment can be incorporated into this type of enzyme/substrate modeling. A comprehensive model for the study of O_2^-–CuZn reaction kinetics at normal or elevated levels of superoxide production needs to be developed to characterize cell reactions to oxidative stress.

The data presented in this report describe quantitative enzyme distribution on intact cell structures where interorganelle relationships are not disturbed. With the knowledge of intracellular SOD concentrations at specific subcellular sites, one can analyze the intracellular relationships between superoxide and SOD; i.e., the rate of O_2^- production in normal cells and the variations in the distribution of SOD molecules in response to different rates of O_2^- production. It is also possible to definitively correlate in vitro enzyme–substrate studies with reliable data regarding in vivo enzyme concentrations.

The authors thank Patricia Upton, Robert Nielsen, Ada Baars, Janice Griffiths, Tom van Rijn, Maurits Niekerk, and Barbara Stockstill for their skilled assistance.

This work was supported in part by National Institutes of Health grant P01 HL31992 PPG and by a grant from RJR Nabisco, Inc.

Received for publication 13 August 1987, and in revised form 3 August 1988.

References

1. Ahlberg, J., L. Marzella, and H. Glaumann. 1982. Uptake and degradation of proteins by isolated rat liver lysosomes: suggestion of a microautophagic pathway of proteolysis. *Lab. Invest.* 97:523–532.
2. Alberts, B., D. Bray, J. Lewis, M. Raff, K. Roberts, and J. D. Watson. 1983. Molecular Biology of the Cell. Gonland Publishing Inc., New York and London. 319–384.
3. Allison, S. A., S. H. Northrup, and J. A. McCammon. 1986. Simulation of biomolecular diffusion and complex formation. *Biophys. J.* 49:167–175.
4. Blouin, A., R. P. Bolender, and E. R. Weibel. 1977. Distribution of organelles and membranes between hepatocytes and nonhepatocytes in the rat liver parenchyma. A stereological study. *J. Cell Biol.* 72:441–455.
5. Bolender, R. P., D. Paumgartner, G. Losa, D. Muellener, and E. R. Weibel. 1978. Integrated stereological and biochemical studies on hepatocytic membranes. I. Membrane recoveries in subcellular fractions. *J. Cell Biol.* 77:565–583.
6. Borst, P. 1986. How proteins get into microbodies (peroxisomes, glyoxysomes, glycosomes). *Biochem. Biophys. Acta.* 866:179–203.
7. Crapo, J. D., and J. M. McCord. 1976. Oxygen-induced changes in pulmonary superoxide dismutase assayed by antibody titrations. *Am. J. Physiol.* 231:1196–1203.
8. Crapo, J. D., and D. Tierney. 1976. Superoxide dismutase and pulmonary oxygen toxicity. *Am. J. Pathol.* 226:1401–1407.
9. Crapo, J. D., B. E. Barry, H. A. Foscue, and J. Shelburne. 1980. Structural and biochemical changes in rat lungs occurring during exposure to lethal and adaptive doses of oxygen. *Am. Rev. Respir. Dis.* 122:123–143.
10. Crapo, J. D., J. M. McCord, and I. Fridovich. 1978. Superoxide dismutases: preparation and assay. *Methods Enzymol.* 53:382–393.
11. Cutler, R. G. 1982. Antioxidants, aging, and longevity. *In* Free Radicals in Biology. W. A. Pryor, editor. Academic Press, New York. 371–428.
12. Forman, H. J., and I. Fridovich. 1973. On the stability of bovine superoxide dismutase. The effect on metals. *J. Biol. Chem.* 248:2645–2649.
13. Freeman, B. A., and J. D. Crapo. 1982. Biology of disease: free radicals and tissue injury. *Lab. Invest.* 47:412–426.
14. Freeman, B. A., S. L. Young, and J. D. Crapo. 1983. Liposome-mediated augmentation of superoxide dismutase in endothelial cells prevent oxygen injury. *J. Biol. Chem.* 258:12534–12542.
15. Geller, B. L., and D. R. Winge. 1982. Rat liver Cu,Zn-Superoxide Dismutase: subcellular location in lysosomes. *J. Biol. Chem.* 257:8945–8952.
16. Gregory, E. M., and I. Fridovich. 1973. The induction of superoxide dismutase by molecular oxygen. *J. Bacteriol.* 114:543–548.
17. Gregory, E. M., and I. Fridovich. 1973. Oxygen toxicity and the superoxide dismutase. *J. Bacteriol.* 114:1193–1197.
18. Gregory, E. M., S. A. Goscin, and I. Fridovich. 1974. Superoxide dismutase and oxygen toxicity in a eukaryote. *J. Bacteriol.* 117:456–460.
19. Griffiths, G., and H. Hoppeler. 1986. Quantitation in immunocytochemistry: correlation of immunogold labeling to absolute number of membrane antigens. *J. Histochem. Cytochem.* 34:1389–1398.
20. Griffiths, G., R. Brands, B. Burke, D. Louvard, and G. Warren. 1982. Viral membrane proteins acquire galactose in *trans* Golgi cisternae during intracellular transport. *J. Cell Biol.* 95:781–792.
21. Harman, D. 1982. The free-radical theory of aging. *In* Free Radicals in Biology. W. A. Pryor, editor. Academic Press, New York. 255–275.
22. Hawco, F., L. Hulett, and P. J. O'Brien. 1980. Hydroxyl radical formation during P_{450} function and benzopyrene hydroxylation. *In* Microsomes, Drug Oxidation and Chemical Carcinogenists. R. W. Estabrook, editor. Academic Press, New York. 419–422.
23. Ho, Y.-S., and J. D. Crapo. 1987. cDNA and deduced amino acid sequence of rat copper-zinc containing superoxide dismutase. *Nucleic Acids Res.* 15:6746.
24. Kikkawa, Y., S. Yano, and L. Skoza. 1984. Protective effect of interferon

inducers against hyperoxic pulmonary damage. *Lab. Invest.* 50:62–71.
25. Klug, D., J. Rabani, and I. Fridovich. 1972. A direct demonstration of the catalytic action of superoxide dismutase through the use of pulse radiolysis. *J. Biol. Chem.* 247:4839–4842.
26. Mansour, H., M. Brun-Pascaud, C. Marquetty, M. Cougerot-Pocidalo, J. Hakin, and J. Pocidalo. 1988. Protection of rat oxygen toxicity by inducers of cytochrome P_{450} system. *Am. Rev. Respir. Dis.* 137:688–694.
27. McCord, J. M. 1985. Oxygen-derived free radicals in postischemic tissue injury. *N. Engl. J. Med.* 312:159–163.
28. McCord, J. M., B. B. Keele, and I. Fridovich. 1971. An enzyme-based theory of obligate anaerobiosis: the physiological function of superoxide dismutase. *Proc. Natl. Acad. Sci. USA.* 68:1024–1027.
29. Lazarow, P. B., and Y. Fujiki. 1985. Biogenesis of peroxisomes. *Annu. Rev. Cell Biol.* 1:489–530.
30. Padmanabhan, R. V., R. Gudaparty, I. E. Liener, B. A. Schwarts, and J. R. Hoidal. 1985. Protection against pulmonary oxygen toxicity in rats by the intratracheal administration of liposome-encapsulated superoxide dismutase or catalase. *Am. Rev. Respir. Dis.* 132:164–167.
31. Peeters-Joris, C., A.-M. Vandevoorde, and P. Baudhuin. 1975. Subcellular localization of superoxide dismutase in rat liver. *Biochem. J.* 150:31–39.
32. Porter, J., M. Sweeney, and E. M. Porter. 1964. Human hepatocuprein: isolation of a copper protein from the subcellular soluble fraction of adult human liver. *Arch. Biochem. Biophys.* 105:319–325.
33. Posthuma, G., J. W. Slot, and H. J. Geuze. 1984. Immunocytochemical assays of amylase and chymotrypsinogen in rat pancrease secretory granules. *J. Histochem. Cytochem.* 32:1028–1034.
34. Posthuma, G., J. W. Slot, and H. J. Geuze. 1987. The usefulness of the immunogold technique in quantitation of a soluble protein in ultrathin sections. *J. Histochem. Cytochem.* 35:405–410.
35. Posthuma, G., J. W. Slot, T. Veenendaal, and H. J. Geuze. 1988. Immunogold determination of amylase concentrations in pancreatic subcellular compartments. *Eur. J. Cell Biol.* 46:327–335.
36. Rajagopalan, K. V. 1980. Xanthine oxidase and aldehyde oxidase. *In* Enzymatic Basis of Detoxication. Vol. 1. W. Jakoby, editor. Academic Press, New York. 295–309.
37. Richardson, J. S., K. A. Thomas, B. H. Rubin, and D. C. Richardson. 1975. Crystal structure of bovine CuZn superoxide dismutase at 3°A resolution:chain tracing and metal legends. *Proc. Natl. Acad. Sci. USA.* 72:1349–1353.
38. Sawada, Y., T. Ohyama, and I. Yamazaki. 1972. Preparation and physiochemical properties of green pea superoxide dismutase. *Biochim. Biophys. Acta.* 268:305–312.
39. Scherle, W. 1970. A simple method for volumetry of organs in quantitative stereology. *Mikroskopie.* 26:57–60.
40. Sharp, K., R. Fine, and B. Honig. 1987. Computer simulation of the diffusion of a substrate to an active site of an enzyme. *Science (Wash. DC).* 236:1460–1463.
41. Shatz, G. 1981. The biogenesis of mitochondria. *In* Mitochondria and Microsomes. C. P. Lee, G. Shatz, and G. Dallner, editors. Addison-Wesley Publishing Co., London, 45–66.
42. Sjostrom, K., and J. D. Crapo. 1983. Structural and biochemical adaptive changes in rat lungs after exposure to hypoxia. *Lab. Invest.* 48:68–79.
43. Slot, J. W., and H. J. Geuze. 1982. Ultracryotomy of polyacrelamide-embedded tissue for immunoelectron microscopy. *Biol. Cell.* 44:325–328.
44. Slot, J. W., and H. J. Geuze. 1984. Gold markers for single and double immunolabeling of ultrathin cryosections. *In* Immunoblotting for Electron Microscopy. J. M. Polak and I. M. Varndell, editors. Elsevier Science Publishers, Amsterdam. 129–142.
45. Slot, J. W., and H. J. Geuze. 1985. A new method of preparing gold probes for multiple-labeling cytochemistry. *Eur. J. Cell Biol.* 38:87–93.
46. Slot, J. W., H. J. Geuze, B. A. Freeman, and J. D. Crapo. 1985. Intracellular localization of the copper-zinc and manganese superoxide dismutases in rat liver parenchymal cells. *Lab. Invest.* 55:363–371.
47. Tainer, J. A., E. D. Getzoff, J. S. Richardson, and D. C. Richardson. 1983. Structure and mechanism of copper-zinc superoxide dismutase. *Nature (Lond.).* 306:284–287.
48. Timcenko-Youssef, L., R. K. Yamazaki, and T. Kimura. 1985. Subcellular localization of adrenal cortical glutathione peroxidase and protective role of mitochondrial enzyme against lipid peroxidative damage. *J. Biol. Chem.* 260:13355–13359.
49. Tokuyasu, K. T. 1980. Immunocytochemistry on ultrathin frozen sections. *Histochem. J.* 12:381–403.
50. Turrens, J. F., and A. Boveris. 1980. Generation of superoxide anion by the NADH dehydrogenase of bovine heart mitochondria. *Biochem. J.* 191:421–427.
51. Turrens, J. F., J. D. Crapo, and B. A. Freeman. 1984. Protection against oxygen toxicity by intravenous injection of liposome-entrapped catalase and superoxide dismutase. *J. Clin. Invest.* 73:87–95.
52. Turrens, J. F., B. A. Freeman, and J. D. Crapo. 1982. Hyperoxia increases H_2O_2 release by lung mitochondria and microsomes. *Arch. Biochem. Biophys.* 217:411–421.
53. Turrens, J. F., B. A. Freeman, J. G. Levitt, and J. D. Crapo. 1982. The effect of hyperoxia on superoxide production by lung submitochondrial particles. *Arch. Biochem. Biophys.* 217:401–410.
54. Van Loon, A. P. G. M., B. Pesold-Hurt, and G. Schatz. 1986. A yeast mutant lacking mitochondrial manganese-superoxide dismutase is hypersensitive to oxygen. *Proc. Natl. Acad. Sci. USA.* 83:3820–3824.
55. Weibel, E. R. 1979. Stereological Methods. Vol. 1. Academic Press, New York.
56. Weisiger, R. A. 1973. The superoxide dismutases from chicken liver: organelle specificity. New evidence for the symbiotic origin of mitochondria. Ph.D. Thesis, Duke University, Durham, NC. 194 pp.
57. Weisiger, R. A., and I. Fridovich. 1973. Superoxide dismutase: organelle specificity. *J. Biol. Chem.* 248:3583–3592.
58. Winkler, J. R., and H. L. Segal. 1984. Swainsonine inhibits glycoprotein degradation by isolated rat lysosomes. *J. Biol. Chem.* 259:15369–15372.
59. Yusa, T., J. S. Beckman, J. D. Crapo, and B. A. Freeman. 1987. Hyperoxia increases hydrogen peroxide production by brain in vivo. *J. Appl. Physiol.* 63:353–358.
60. Yusa, T., J. D. Crapo, and B. A. Freeman. 1984. Hyperoxia enhances lung and liver nuclear superoxide generation. *Biochim. Biophys. Acta.* 798: 167–174.